mathematics

MDPI

Article

Fault Detection and Isolation Strategy for Brake Actuation Units of High-Speed Trains Under Variable Operating Conditions

Jingxian Ding [1,2,*], Tianyu Xia [2], Xinzhou Wu [2], Shize Zheng [2] and Tianyi Wang [2]

[1] Postdoctoral Station of Mechanical Engineering, Tongji University, Shanghai 201804, China
[2] College of Transportation, Tongji University, Shanghai 201804, China
* Correspondence: dingjx@tongji.edu.cn

Abstract: The brake system is a key system for the safe operation and stopping of trains. As a core component of brake systems, the brake actuation unit (BAU) is essential for slowing down or stopping trains, and faults in the BAU will affect the safety and efficiency of train operation. In order to detect and locate faults in the BAU in time, a fault detection and isolation (FDI) strategy, based on mutual residuals (MRs), principal component analysis (PCA) and improved reconstruction-based contribution plots (IRBCP), was proposed. Firstly, the structural composition and working principle of the BAU were introduced, and its typical failure modes and effects were analyzed. Secondly, considering that the fault detection threshold is not easy to determine due to the variable operating conditions of the BAU, the steady-state fault feature based on MR was extracted. Thirdly, fault detection and isolation were realized based on PCA and the IRBCP algorithm. Finally, by using the fault injection method, case studies on test-rig experiment data of brake systems were conducted; the fault detection rate was 99% and the effectiveness of the proposed strategy was validated by the test data. The proposed strategy shows fast computing ability, and is suitable for systems with dynamic time-varying and nonlinear characteristics.

Keywords: brake system; brake actuation unit; fault detection; fault isolation; time-varying system

MSC: 93C10

check for updates

Academic Editor: Zhijia Zhao

Received: 9 February 2025
Revised: 17 March 2025
Accepted: 18 March 2025
Published: 21 March 2025

Citation: Ding, J.; Xia, T.; Wu, X.; Zheng, S.; Wang, T. Fault Detection and Isolation Strategy for Brake Actuation Units of High-Speed Trains Under Variable Operating Conditions. *Mathematics* **2025**, *13*, 1022. https://doi.org/10.3390/math13071022

Copyright: © 2025 by the authors. Licensee MDPI, Basel, Switzerland. This article is an open access article distributed under the terms and conditions of the Creative Commons Attribution (CC BY) license (https://creativecommons.org/licenses/by/4.0/).

1. Introduction

With the continuous development of rail transit networks, a large number of trains have been put into service. Their characteristics of high speed, large capacity and long service time determine the extremely high importance of safety and reliability for the equipment of trains, which have received widespread attention [1,2]. As a key component for the safety of trains, the brake system plays a vital important role in slowing down or stopping trains. The brake actuation unit (BAU), the actuator of the brake system, suffers from vibration agitation and sand and dust intrusion, as well as electromagnetic interference. As a result, the performance degradation of components in the BAU will inevitably occur, which can consequently cause braking not being relieved, insufficient brake force, etc., affecting the operation safety, efficiency and maintenance costs of trains. Fault diagnosis (FD) is an effective way to improve the system's active safety ability and reduce accident risk [3].

Generally, FD methods can be classified into three types: analytical-model-based [4,5], knowledge-based [6] and signal-processing-based [7]. With the emergence and widespread application of emerging diagnostic methods, such as machine learning and deep learning,

studies on the FD of brake systems have been increasingly conducted in recent years [8]. Niu [9] proposed an FDI method for locomotive brake systems based on bond graph models. Zuo [10] established a performance degradation monitoring model based on a data fusion method for pneumatic brake systems. Lu [11] proposed a data-driven approach for sensor fault detection and diagnosis of an electropneumatic brake system. Niu [12] investigated a fault detection isolation and diagnosis strategy of speed sensors for high-speed trains, based on PCA and reconstruction-based contribution plots (RBCP). Zuo [13] proposed a multi-source information fusion method based on Kalman filter (KF), the sequential probability ratio test (SPRT) and support vector classification (SVC) for the latent leakage fault identification and diagnosis of key pneumatic units in electric multiple unit (EMU) brake systems. Zhou [14] proposed an FDI method for EMU brake cylinder systems based on intervariable variance (IVV) and RBCP. Seo [7] conducted fault diagnosis for the solenoid valve of railway brake systems with embedded sensor signals and physical interpretation. Sang [15] carried out research on incipient fault detection for the air brake systems of high-speed trains. Ji [16,17] proposed a combined indicator to detect and diagnose incipient sensor faults. It can be found from the current literature that there have been many studies on the fault diagnosis of brake systems but few studies on the FDI of BAUs. In the meantime, because of the time-varying characteristics, the signal of BAUs is non-smooth. The fault detection threshold of current threshold logic judgment methods lacks a sufficient theoretical basis, and few studies on the FDI of BAUs under variable operating conditions have been conducted.

In this paper, an FDI strategy for BAUs based on mutual residuals (MRs), principal component analysis (PCA) and improved reconstruction-based contribution plots (IRBCP) is proposed. The strategy considers brake cylinder pressure signals from four axles of a vehicle simultaneously, and the MR of these signals is extracted. A PCA monitoring model is developed by using the normal brake cylinder pressure data from the four axles, and statistical thresholds are defined. Combined statistics derived from the PCA monitoring model are compared with statistical thresholds to detect faults. To pinpoint the fault location, the reconfiguration contribution of each variable is calculated for all fault moments, and the IRBCP algorithm is proposed. The proposed strategy has a simple algorithm and fast computing ability and is practically suitable for systems with dynamic time-varying nonlinear characteristics. Moreover, the strategy extends the usage of PCA.

The remaining parts of this paper are organized as follows. Section 2 introduces the brake system and the failure modes and effects of the BAU. Section 3 presents the FDI strategy. Section 4 describes some case studies to demonstrate the effectiveness of the proposed strategy. Finally, conclusions are drawn in Section 5, with some perspectives on research and development.

2. Brake Systems and FMEA of the BAU

2.1. Brake Systems

The brake force of trains consists of the electric brake force and the air friction brake force. The electric brake force generated by the traction motor diminishes as the train's speed decreases, while the air friction brake force is supplied by the air brake system. The air brake system is activated during service brake and emergency brake at low speeds, as well as urgent brake. As a result, the air brake system has been used as the indispensable safety system for decelerating or stopping trains.

As shown in Figure 1a, the microcomputer-controlled electropneumatic brake system is widely used in trains, and it mainly includes the driver controller, the electronic brake control unit (EBCU), the pneumatic brake control unit (PBCU), and the brake actuation unit (BAU). The driver controller generates brake command signals and transmits them to the

EBCU for brake force calculation and distribution. The PBCU generates relay valve output pressure, i.e., P_{BC}, according to the instructions of the EBCU, i.e., I_{EP}. The BAU transfers the brake cylinder pressure into the mechanical brake force.

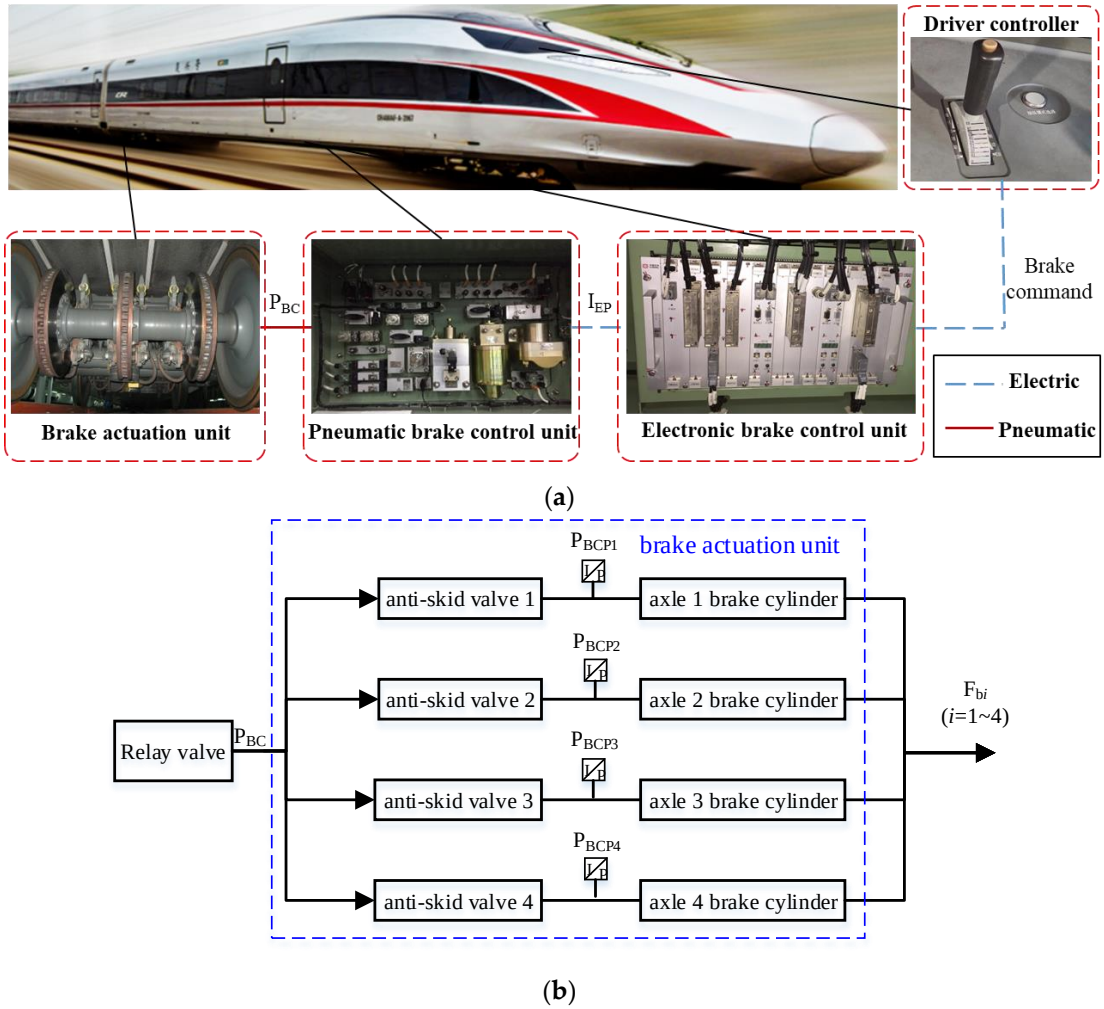


Figure 1. Brake systems and the brake actuation unit. (**a**) Composition of brake systems; (**b**) schematic diagram of the brake actuation unit.

2.2. Working Principle of the Brake Actuation Unit

The brake actuation unit, as the actuating part of brake systems, primarily consists of anti-skid valves, axle brake cylinders, brake cylinder pressure sensors and brake pipes on four axles.

As shown in Figure 1b, the input of the BAU is the output pressure of the relay valve, i.e., P_{BC}, and the axle brake cylinder pressure on four axles is derived from the same relay valve. Therefore, in the absence of anti-skid control and the failure of the BAU, the pressures of the axle brake cylinders on four axles should be basically consistent.

2.3. Failure Modes and Effects Analysis of the BAU

Despite the components included in the BAU having a high reliability, the BAU is still susceptible to failures due to ageing and wear of rubber seals, contamination of compressed air and electromagnetic interference due to the harsh working environment. It can lead to stalling of the anti-skid valve spool, leakage or blockage in brake cylinders and brake pipes, and abnormal output signals of pressure sensors. These failures can cause performance degradation of the brake system, such as slow response and reduced control accuracy,

and even function failures, such as braking not being relieved and insufficient brake force. By analyzing the work principle and physical structure of the BAU, main failure modes, mechanisms and effects are summarized in Table 1.

Table 1. Failure modes, mechanisms and effects of the BAU.

Component	Failure Modes	Failure Mechanisms	Failure Effects
Anti-skid valve	Leakage	Ageing and wear of rubber seals	Low brake cylinder pressure, thus causing insufficient brake force
	Blockage	Contamination of compressed air	Slow rising and falling of the brake cylinder pressure, thus causing insufficient brake force and braking not being relieved
Brake cylinder	Blockage	Contamination of compressed air	Slow rise and fall of the brake cylinder pressure, thus causing insufficient brake force and braking not being relieved
	Leakage	Ageing and wear of rubber seals	Reduced brake cylinder pressure, thus causing insufficient brake force
Brake pipe	Leakage	Ageing and wear of rubber seals	Reduced brake cylinder pressure, thus causing insufficient brake force
Pressure sensor	Noise	Electromagnetic interference	Large fluctuations of the brake cylinder pressure, thus causing inaccurate brake force control
	Bias	Fatigue failure of solder joints of the internal circuit board or broken connection cables	High or low brake cylinder pressure, thus causing inaccurate brake force control
	Drift	Ageing of electronic components due to high temperatures	Slow changes in the brake cylinder pressure over time, thus causing inaccurate brake force control

As indicated in Table 1, the main failure effects of the BAU are manifested through abnormal brake cylinder pressures. Brake cylinder pressure is an important variable to reflect the performance of air brake systems [10], and it serves as the foundation for anti-skid and brake force control. Therefore, monitoring the axle brake cylinder pressure of each axle can effectively facilitate fault detection of the BAU. Meanwhile, since there are multiple axle brake cylinder pressure signals involved, fault detection of the BAU falls within the realm of multivariate statistical process monitoring.

Common multivariate statistical analysis methods include principal component analysis, partial least squares and independent principal component analysis. Among them, principal component analysis (PCA) has emerged as the most widely used method for process monitoring, largely due to its simple algorithm and robust convergence properties [18]. Actually, the brake system exhibits a three-state characteristic of braking, holding, and relief, and the brake cylinder pressure is influenced by factors such as stage, speed and load. As a result, the axle brake cylinder pressure varies with changing operating conditions, which does not align well with the assumptions required for PCA [19]. Therefore, it is necessary to extract steady-state fault features from the axle brake cylinder pressure signals of the BAU.

3. Fault Detection and Isolation Strategy of the BAU

The flowchart of the FDI strategy of the BAU is shown in Figure 2.

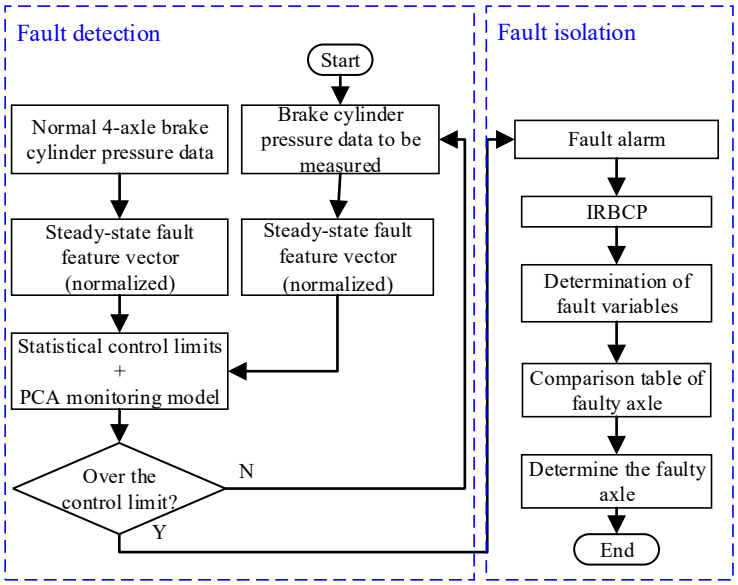


Figure 2. The flowchart of the FDI strategy of the BAU.

3.1. Fault Feature Extraction for the BAU

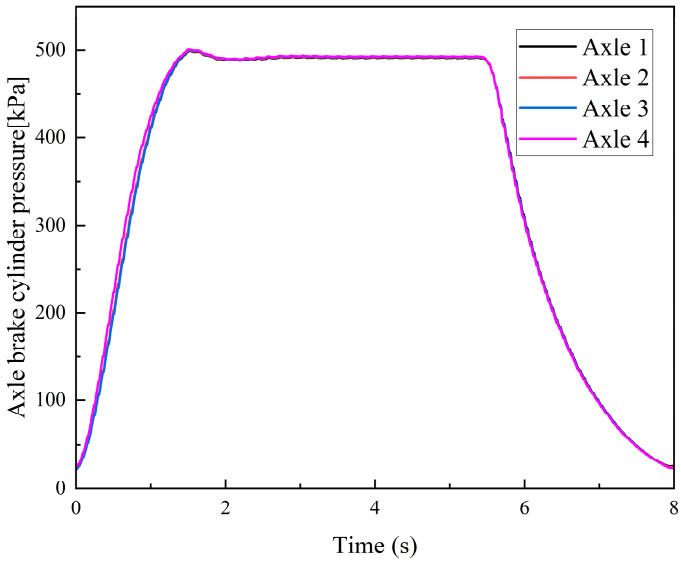
Aimed at the non-smooth and non-gaussian characteristics, the mutual residuals (MR) among the axle brake cylinder pressure of four axles is extracted to construct a steady-state fault feature vector.

For a vehicle with k axles, MR is expressed as:

$$\mathrm{MR}_{i-j} = ABCP_i - ABCP_j, i, j \in \{1, 2, \cdots, k\}; i < j, \tag{1}$$

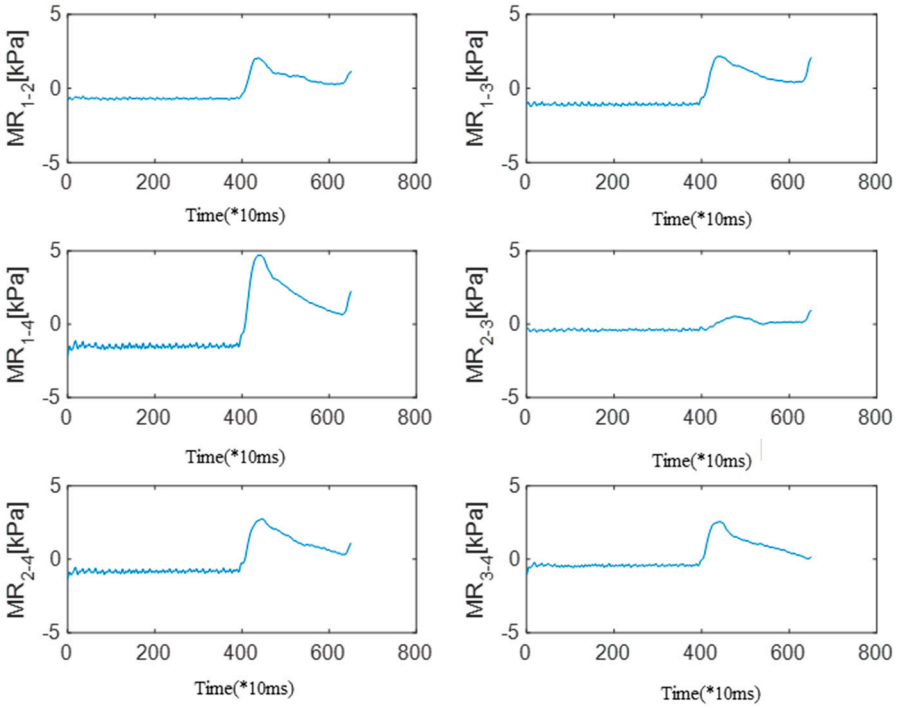
where $ABCP_i$ and $ABCP_j$ are the axle brake cylinder pressures on the ith and jth axle.

For the axle brake cylinder pressures of four axles of the BAU under normal conditions, as shown in Figure 3a, MR curves of the BAU can be calculated according to Equation (1), as shown in Figure 3b.



(**a**)

Figure 3. *Cont.*



(**b**)

Figure 3. Brake cylinder pressures of four axles and MR curves of the BAU under normal conditions. (**a**) Brake cylinder pressures of four axles of the BAU under normal conditions; (**b**) MR curves of the BAU under normal conditions (corresponding to 1.5 s to 8 s in Figure 3a).

As shown in Figure 3b, the MR of the BAU is small under normal conditions, fluctuating around 0, and signals are approximately steady-state. Meanwhile, the absolute value of MR is no more than 5 kPa at most, which is lower than the detection threshold set by the self-diagnostic equipment of the brake system of in-service trains. Therefore, a large MR during the service period of the brake system can warn of an abnormality or failure of the BAU. In addition, a Quantile–Quantile (Q-Q) plot [12] of the MR of the BAU under normal conditions is plotted, as shown in Figure 4.

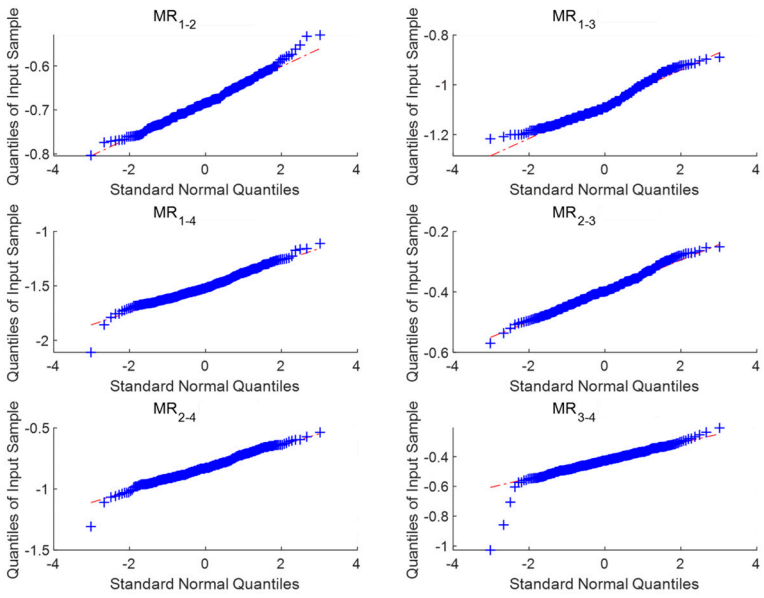


Figure 4. Q-Q plot of the MR of the BAU under normal conditions.

As can be seen from Figure 4, the sample data in the Q-Q plot of the MR of the BAU under normal conditions are basically approximated to be on a straight line, which further indicates that the steady-state fault feature vector constructed in this paper is approximately gaussian distributed, i.e., they satisfy the conditions of use of PCA-based fault detection [12,18].

3.2. Fault Detection of the BAU Based on PCA

As a fault detection method based on multivariate statistical analysis, PCA is able to detect faults by using the correlation between data. By analyzing historical data collected under normal operating conditions, the principal components that can express the relationships between the brake cylinder pressure signals of the four axles are extracted; then, a PCA monitoring model of the BAU is established. Meanwhile, a detection statistic is defined, and its control limit under normal operating conditions is determined. When the detection statistic of the sample data to be measured exceeds the control limit, the BAU is flagged as faulty.

3.2.1. Steady-State Fault Feature Vector Extraction

Let $X \in R^{n \times m}$ represent the training sample matrix of the steady-state fault feature vector under normal operating conditions.

$$X = \begin{bmatrix} x_{11} & x_{12} & \cdots & x_{1m} \\ x_{21} & x_{22} & \cdots & x_{2m} \\ \vdots & \vdots & \ddots & \vdots \\ x_{n1} & x_{n2} & \cdots & x_{nm} \end{bmatrix}, \tag{2}$$

where m is the number of variables in the BUA and n is the number of training samples.

X is normalized by z-score [20] to obtain the normalization matrix Y, and the covariance matrix of Y is expressed as:

$$S = \frac{1}{n-1} Y^T * Y, \tag{3}$$

3.2.2. Determining the Number of Principal Components

Solving the characteristic equation of S, m eigenvalues of $\lambda_1, \lambda_2, \cdots, \lambda_m$ ($\lambda_1 \geq \lambda_2 \geq \cdots \geq \lambda_m \geq 0$) and the corresponding eigenvectors ($p_1, p_2, \cdots, p_m$) can be obtained.

The cumulative variance contribution method [21] is adopted to determine a:

$$Contr(p_a) = \frac{\sum_{j=1}^{a} \lambda_j}{\sum_{j=1}^{m} \lambda_j}, \tag{4}$$

where a is the number of principal components and $a \leq m$.

In this paper, when $Contr(p_a)$ is larger than 85%, it indicates that the information contained in the first a principal component has reached the required information to represent the original m variables, and the number of principal components is a.

3.2.3. Building a PCA Monitoring Model

Based on the first a principal components, corresponding eigenvalues $\lambda_1, \lambda_2, \cdots, \lambda_a$, and the eigenvector $P = (p_1, p_2, \cdots, p_a)$, the PCA monitoring model of the BAU is established as follows:

$$\begin{aligned} &\hat{Y} = TP^T \\ &= \sum_{i=1}^{a} t_i p_i^T \\ &= Yp_1 p_1^T + Yp_2 p_2^T + \cdots + Yp_a p_a^T, i = 1, 2, \cdots, a \end{aligned}, \tag{5}$$

where $\hat{Y}$ is the principal subspace, $T = [t_1, t_2, \cdots, t_a] \in R^{n \times a}$ is the principal score matrix and $T = YP$, $P = [p_1, p_2, \cdots, p_a]$ is the load matrix.

3.2.4. Combined Statistic

From a statistical point of view, FD of the BAU involves the process of constructing statistics in both the principal subspace and the residual subspace to perform statistical hypothesis testing. The samples to be tested are projected onto these two subspaces, and the statistics are compared with the predefined threshold to judge the state of the BAU. The two most commonly used statistics in this context are the T^2 statistic and the Squared Prediction Error (*SPE*) statistic.

Multiple principal score vectors are monitored simultaneously by calculating the T^2 statistic:

$$\begin{aligned} T^2 &= t\Lambda^{-1}t^T \\ &= xP \cdot \Lambda^{-1} \cdot P^T x^T \end{aligned}, \tag{6}$$

where $\Lambda = diag\{\lambda_1, \lambda_2, \cdots, \lambda_a\}$.

The control limit of the T^2 statistic is determined as:

$$T_\alpha^2 = \frac{a(n^2-1)}{n(n-a)} \cdot F_\alpha(a, n-a), \tag{7}$$

where $F_\alpha(a, n-a)$ is the threshold of the F distribution with degrees of freedom a, $n-a$ and a confidence level of α.

The *SPE* statistic is calculated as:

$$SPE = x(I - PP^T)(I - PP^T)^T x^T = \left\| (I - PP^T)x \right\|^2, \tag{8}$$

The control limit of the *SPE* statistic is calculated as:

$$\delta_\alpha^2 = \theta_1 \left[\frac{c_\alpha h_0 \sqrt{2\theta_2}}{\theta_1} + 1 + \frac{\theta_2 h_0 (h_0 - 1)}{\theta_1^2} \right]^{\frac{1}{h_0}}, \tag{9}$$

$$\theta_i = \sum_{j=a+1}^{m} \lambda_j^i, i = 1, 2, 3, \tag{10}$$

$$h_0 = 1 - \frac{2\theta_1 \theta_3}{3\theta_2^2}, \tag{11}$$

where c_α is the threshold for a confidence level of α under the standard normal distribution, which can be obtained by consulting the standard normal distribution table, and a $\delta 2$ confidence limit of 99% is taken in this paper [12].

According to [22], the *SPE* statistic is more sensitive to faults than the T^2 statistic; however, there are inconsistencies in practical applications due to their different magnitudes ($T^2 > SPE$). A combined statistic that incorporates the T^2 and the *SPE* is used in this paper, which is expressed as:

$$\varphi(x) = \frac{T^2}{T_\alpha^2} + \frac{SPE}{\delta_\alpha^2} = x^T \phi x, \tag{12}$$

where ϕ is expressed as:

$$\phi = \frac{P\Lambda^{-1}P^T}{T_\alpha^2} + \frac{I - PP^T}{\delta_\alpha^2}, \tag{13}$$

The control limit of the $\varphi(x)$ is calculated as follows:

$$\zeta_\alpha^2 = g\chi_{h,\alpha}^2, \tag{14}$$

$$g = \frac{tr(S\phi)^2}{tr(S\phi)} \tag{15}$$

$$h = \frac{[tr(S\phi)]^2}{tr(S\phi)^2} \tag{16}$$

where g is a coefficient, $\chi^2_{h,\alpha}$ is a χ^2 distribution with h degrees of freedom and a confidence level of α, and $tr(\cdot)$ is the trace of a matrix.

3.3. FDI of the BAU Based on IRBCP

Once an abnormality or fault is detected in the BAU, the moment of fault occurrence is recorded, and further analysis is required to identify the faulty variable and isolate the axle where the fault is located. Contribution plot [23] and reconstruction-based contribution [24] are two classical methods for fault variable identification. The latter overcomes the fault trailing effect present in the contribution plot method, thereby improving the accuracy of single faulty variable identification. However, since the steady-state fault feature vector is constructed by solving the residuals among the brake cylinder pressure signals of four axles of the BAU, a fault of single axle brake cylinder pressure results in three corresponding faulty variables. This creates a typical multiple faulty variables scenario and introduces uncertainty regarding the exact moment of fault occurrence.

In this paper, aiming at the problem of recognizing multiple faulty variables and multiple faulty moments, an improved reconstruction-based contribution plots (IRBCP) algorithm that combines the advantages of the contribution plot method and the reconstruction-based contribution method is proposed, and the specific implementation steps are as shown in Figure 5.

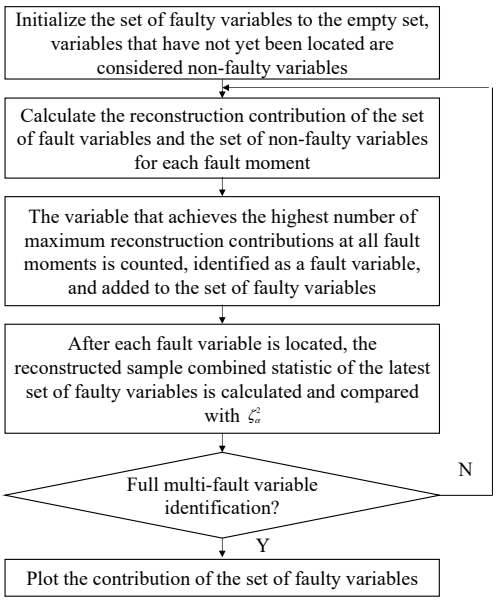


Figure 5. The flowchart of the IRBCP algorithm.

By conducting the IRBCP algorithm, the location of the brake cylinder pressure signal of the faulty axle is achieved according to Table 2.

Table 2. Comparison of faulty variables and the axle brake cylinder pressure involved.

Faulty Variables	Axle Brake Cylinder Pressure Involved
1	axles 1 and 2
2	axles 1 and 3
3	axles 1 and 4
4	axles 2 and 3
5	axles 2 and 4
6	axles 3 and 4

It is worth mentioning that the IRBCP algorithm can effectively avoid the fault trailing effect, as it only calculates the reconstruction contribution rate for the faulty samples.

4. Case Analysis and Validation

4.1. Fault Sample Acquisition

In order to validate the effectiveness of the FDI strategy, considering the limited faulty samples of the BAU as well as the high cost of physical test, a fault injection method [25] is employed. The brake cylinder pressure data under normal condition are obtained from the test-rig of the brake system in Figure 6a, and it is utilized to generate faulty sample data under typical failure modes.

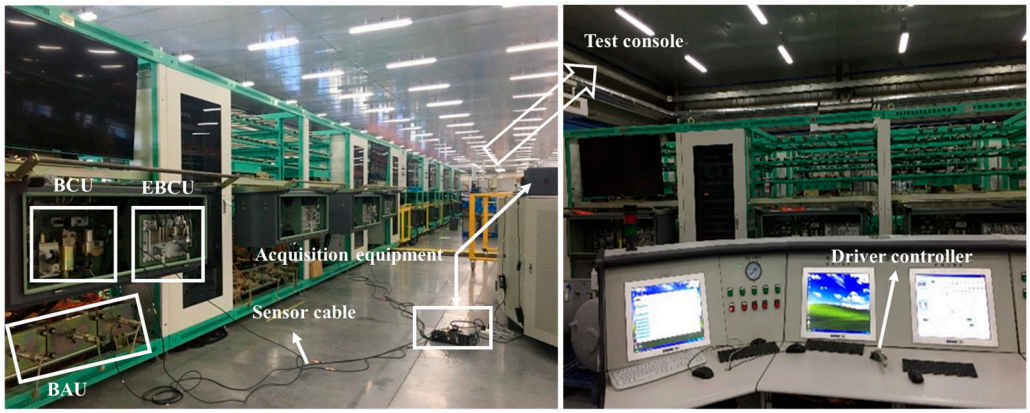
The gas flow area is reduced when the blockage occurs, which can be simulated by connecting small-diameter throttle orifices. The brake cylinder pressure is reduced when leakage occurs, which can be simulated by connecting throttle orifices in parallel and connecting them to the atmosphere. The brake cylinder pressure signal is abnormal when noise, bias and drift occur, which can be simulated by adding the corresponding error to the normal value of the pressure sensor.

In this paper, typical fault injection of bias and drift are conducted.

(1) Injecting a 5 kPa pressure error to the pressure sensor value of axle 3 to simulate a sensor bias fault.

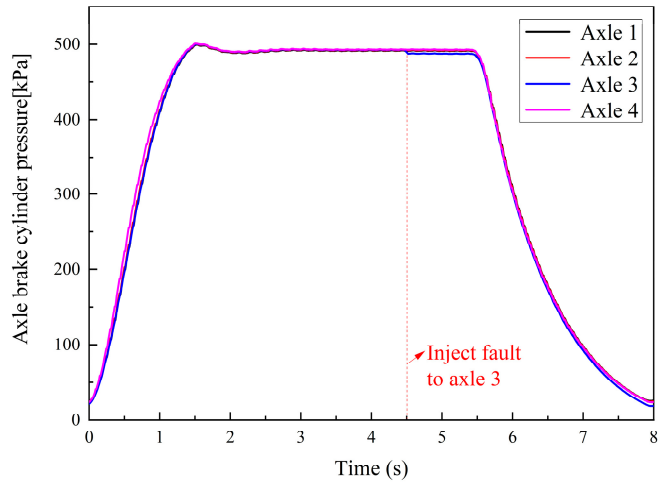
(2) Injecting a 0.15 kPa/s pressure error to the pressure sensor value of axle 4 to simulate a sensor drift fault.

The pressure curves of the BAU under bias and drift faults are obtained in Figure 6b,c.

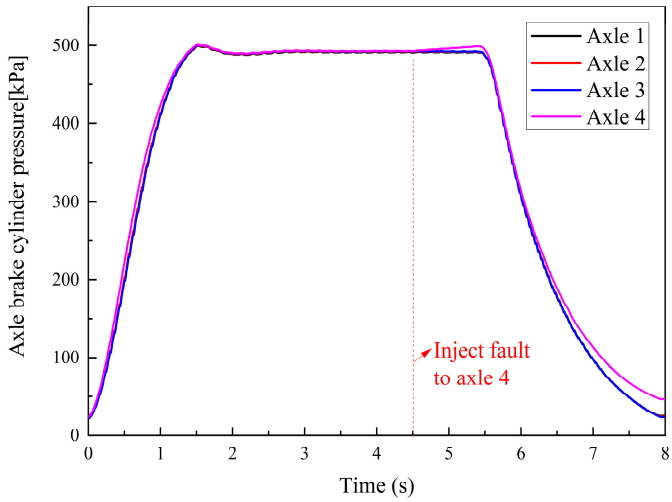


(**a**)

Figure 6. *Cont.*



(**b**)



(**c**)

Figure 6. Fault simulation results of the BAU. (**a**) Test-rig of the brake system; (**b**) bias fault; (**c**) drift fault.

4.2. Fault Detection and Isolation Results

The normal operating data of brake cylinder pressures of four axles in Figure 3a are selected as the training sample to establish the PCA monitoring model of the BAU. The control limit of the combined statistics is calculated as $\zeta(\varphi) = 1.36$. Subsequently, the data under the bias fault condition, depicted in Figure 6b, are used as testing samples. The real-time combined statistics are computed, and the corresponding fault detection results are presented in Figure 7.

As can be seen in Figure 7, the combined statistics of the testing samples exceed the control limit between 2.99 s and 6.5 s, indicating that a fault occurs and can be rapidly detected.

In order to isolate the faulty axle, the IRBCP algorithm is adopted. The reconstructed contribution values of the six MR variables in the steady-state fault feature vector are calculated for each fault moment in turn, and the number of times the RBC maximum is obtained for each variable is counted. The number of times the six MR variables obtained RBC maximum at the first reconstruction are 0, 0, 0, 352, 0 and 0, so the faulty variable at the

first reconstruction is 4. The combined statistics for reconstructed samples are calculated, as shown in Figure 8.

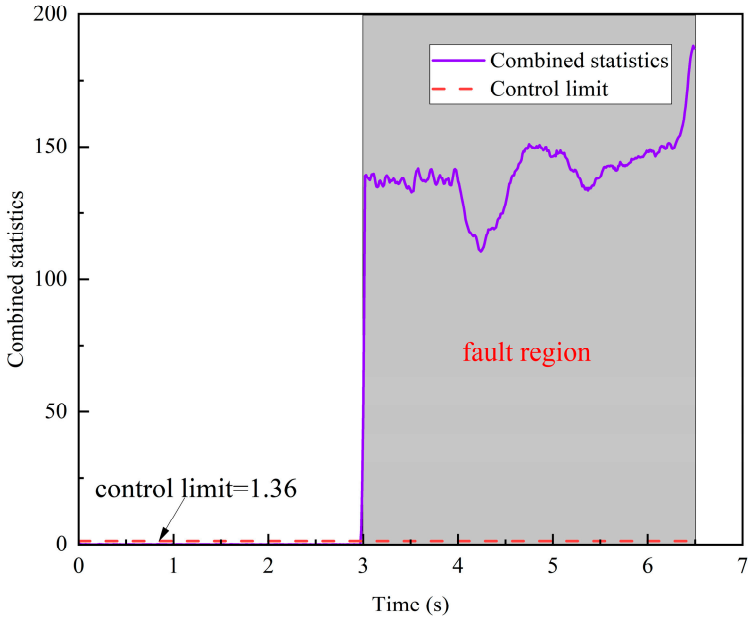


Figure 7. Bias fault detection results (corresponding to the 1.5 s to 8 s in Figure 6b).

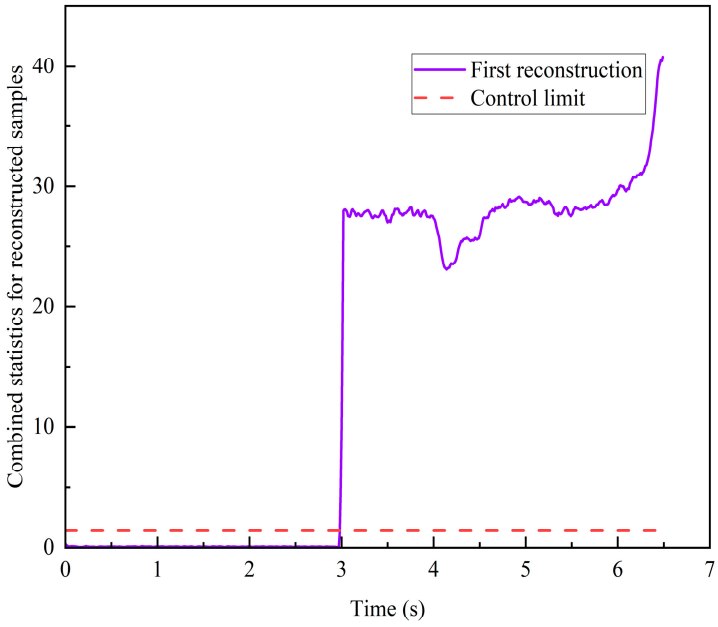


Figure 8. The combined statistics for reconstructed samples after the first reconstruction.

As can be seen in Figure 8, the combined statistics of the reconstructed samples exceed the control limit between 3.0s and 6.5 s, so a second reconstruction is required. The number of times the six MR variables obtained the maximum value of RBC during the second reconstruction are 0, 0, 0, 0, 0 and 352, so the faulty variable is 6. The combined statistics are calculated, as shown in Figure 9.

As can be seen in Figure 9, after the second reconstruction, the combined statistics for reconstructed samples still exceeded the control limit in the range of 3.01s to 6.5 s. Therefore, a third reconstruction is required. At the third reconstruction, the number of times the six MR variables obtained the maximum value of RBC are 0, 352, 0, 0, 0 and 0, so

the faulty variable is 2. As presented in Figure 10, the combined statistics are all below the control limit, and the fault isolation is finished.

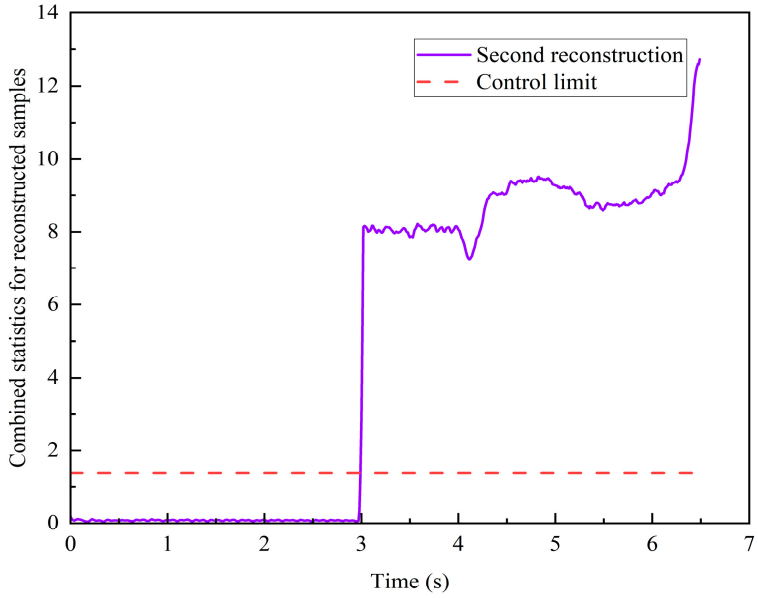


Figure 9. The combined statistics for reconstructed samples after the second reconstruction.

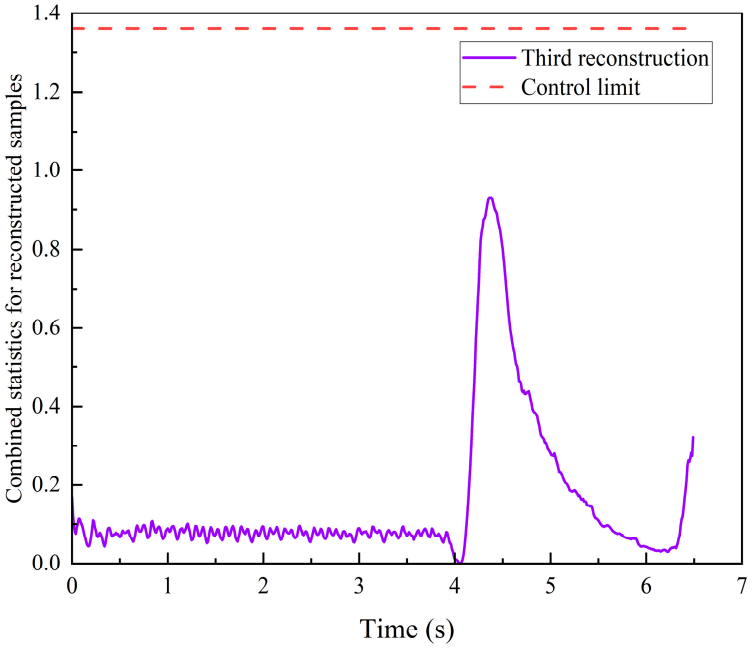


Figure 10. The combined statistics for reconstructed samples after the third reconstruction.

Therefore, the faulty variables of the bias fault are {4, 6, 2}. Under the single-fault assumption, the fault occurs in the third axle according to Table 2, which aligns with the fault injection scenario depicted in Figure 6b. Similarly, the drift fault detection results are shown in Figure 11. The faulty variables of the drift fault are {6, 5, 3}, and the fault occurs in the fourth axle according to Table 2, which further proves the accuracy of the proposed strategy.

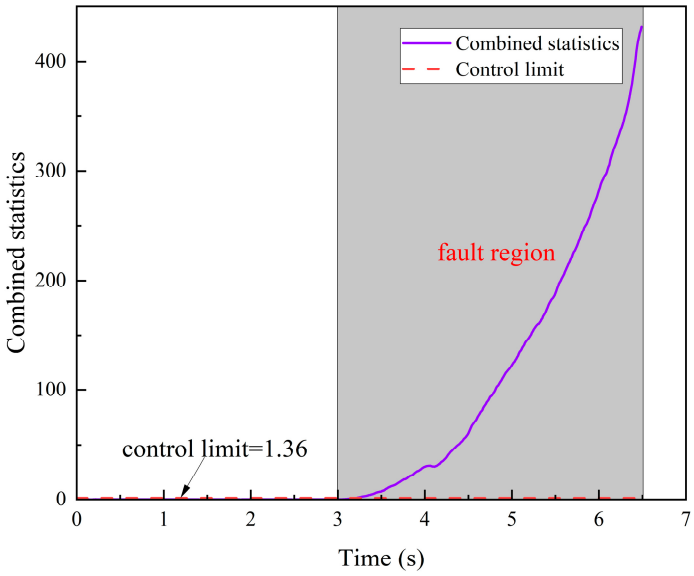


Figure 11. Drift fault detection results (corresponding to the 1.5 s to 8 s in Figure 6c).

4.3. Results Analysis of Comparative Methods

Based on the above analysis of the bias and drift FDI results of the BAU, it can be found that the accuracy of the fault detection results based on the PCA monitoring model is very critical, which directly affects the effectiveness of the subsequent fault isolation. In order to further verify the accuracy of the MR + PCA-based method for fault detection of the BAU, the commonly used fault detection method based on the Kalman filter (KF) state prediction function is selected for comparative validation.

According to [26], the fault detection method based on the traditional KF state prediction function can extract the fault inflection point, but the faults after the fault inflection point cannot be detected effectively. In order to solve this problem, combined with the structural characteristics of the BAU, the new message sequence is reconstructed based on the traditional KF state prediction function, i.e., once a fault inflection point is detected, the faulty signal is replaced by utilizing the optimal state estimation value of the rest of the normal axle brake cylinder pressure of the BAU.

Taking the three-axle bias fault in Figure 6b as an example, the residual between the predicted value based on the reconstructed KF and the observed value of the three-axle brake cylinder pressure is calculated and compared with the preset detection threshold; the correct rates of the two detection methods are counted, as shown in Table 3.

Table 3. Correct detection rate of bias faults.

Detection Method	Number of Missed Detections	Number of False Detections	Correct Rate
reconstructed KF	99	0	72%
MR + PCA	0	2	99%

As can be seen from Table 3, compared with the reconstructed KF, the MR + PCA-based method proposed in this paper has a higher correct detection rate under the same number of faulty samples to be tested. It is also further shown that the statistical threshold constructed by using the normal brake cylinder pressure data of four axles of the BAU is more effective.

5. Conclusions

This paper investigates the FDI strategy for the BAU of high-speed trains.

(1) A fault detection method based on the MR and PCA is developed to tackle the difficulty in setting fault detection thresholds. Specifically, the MR is extracted from brake cylinder pressure signals of four axles to form a steady-state fault feature vector. A PCA monitoring model is then established by using normal brake cylinder pressure data of four axles. By defining a statistical threshold and comparing it with the combined statistics, the method enables real-time fault detection, achieving a fault detection rate of 99%. This approach effectively mitigates the impact of nonlinearity and non-smoothness of brake cylinder pressure signals, which are typically caused by varying operating conditions of the brake system. Additionally, it extends the applicability of PCA in complex industrial monitoring scenarios.

(2) To address the challenges of multiple faulty variables and multiple faulty moments in the BAU, a fault isolation method based on the IRBCP algorithm is proposed. Fault simulation tests are conducted to obtain brake cylinder pressure fault data. The results show that bias and drift faults can be detected in time and the faulty variables can be accurately identified to locate the faulty axle.

(3) The application of this strategy enables the detection and isolation of faults in the BAU, which provides guidance on the repair and replacement of components in the brake system and helps to reduce maintenance costs.

The proposed strategy has a simple algorithm and fast computing ability and is suitable for systems with dynamic time-varying nonlinear characteristics. Despite the above advantages, this paper only considers the single-fault case, and further research should be conducted to investigate the FDI strategy of the BAU under the multi-fault case and the sensitivity of statistical thresholds to noise. Additionally, the use of adaptive thresholds should be discussed.

Author Contributions: Conceptualization, J.D.; Data curation, T.X. and T.W.; Formal analysis, S.Z.; Investigation, X.W.; Methodology, J.D.; Validation, J.D.; Visualization, T.X.; Writing—original draft, J.D. All authors have read and agreed to the published version of the manuscript.

Funding: This research was funded by the Science and Technology Research and Development Programme Topics of China State Railway Group Co., Ltd. (Grant No. N2022J019).

Data Availability Statement: Data are available from the authors upon reasonable request.

Acknowledgments: The authors also thank the CRRC Nanjing Puzhen Haitai Brake Equipment Co., LTD for providing test support.

Conflicts of Interest: The authors declare no conflicts of interest.

References

1. Xing, J.D.; Yang, W.; Yin, X.L.; Zio, E. An integrated method of resilience and risk assessment for maintenance strategy optimization of a train braking system. *Reliab. Eng. Syst. Saf.* **2025**, *260*, 110929.
2. Zuo, J.Y.; Ding, J.X. Research progress on intelligent control and maintenance technology of railway vehicle braking system. *J. Traffic Transp. Eng.* **2021**, *21*, 50–62.
3. Liu, Z.; Zhang, M.; Liu, F.; Zhang, B. Multidimensional feature fusion and ensemble learning-based fault diagnosis for the braking system of heavy-haul train. *IEEE Trans. Ind. Inform.* **2021**, *17*, 41–51.
4. Xiong, L.J.; He, Y.F.; Chen, Y.J.; Lu, J.; Niu, G. Digital twin-based degradation prediction for train electro-pneumatic valve. *Reliab. Eng. Syst. Saf.* **2023**, *240*, 109627.
5. Xu, S.Q.; Yu, H.Y.; Wang, H.; Chai, H.; Ma, M.; Chen, H.; Zheng, W.X. Simultaneous Diagnosis of Open-Switch and Current Sensor Faults of Inverters in IM Drives Through Reduced-Order Interval Observer. *IEEE Trans. Ind. Electron.* **2024**, 1–12. [CrossRef]
6. Ji, H.Q. Optimization-based incipient fault isolation for the high-speed train air brake system. *IEEE Trans. Instrum. Meas.* **2022**, *71*, 3501709.

7. Seo, B.; Jo, S.H.; Oh, H.; Youn, B. Solenoid valve diagnosis for railway braking systems with embedded sensor signals and physical interpretation. In Proceedings of the Annual Conference of the Prognostics and Health Management Society 2016, Denver, CO, USA, 3–6 October 2016; pp. 337–343.
8. Hou, Z.F.; Lee, C.K.M.; Lv, Y.Q.; Keung, K. Fault detection and diagnosis of air brake system: A systematic review. *J. Manuf. Syst.* **2023**, *71*, 34–58.
9. Niu, G.; Zhao, Y.J. Bond Graph Model Based Fault Detection and Isolation for Locomotive Brake. *J. Tongji Univ. (Nat. Sci.)* **2015**, *43*, 894–899.
10. Zuo, J.Y.; Ding, J.X.; Hu, W.; Han, F.; Zhang, L. Performance degradation monitoring based on data fusion method for in-service train pneumatic brake system. *Proc. Inst. Mech. Eng. Part C J. Mech. Eng. Sci.* **2019**, *233*, 1924–1938.
11. Lu, Y.Y.; Fan, X.P.; Gao, D.Z.; Cheng, Y.; Yang, Y.; Zhang, X.; Li, S.; Peng, J. A data-based approach for sensor fault detection and diagnosis of Electro-Pneumatic brake. In Proceedings of the 2019 IEEE International Conference on Prognostics and Health Management, San Francisco, CA, USA, 17–20 June 2019.
12. Niu, G.; Xiong, L.J.; Qin, X.X.; Pecht, M. Fault detection isolation and diagnosis of multi-axle speed sensors for high-speed trains. *Mech. Syst. Signal Process.* **2019**, *131*, 183–198.
13. Zuo, J.Y.; Ding, J.X.; Feng, F.R. Latent leakage fault identification and diagnosis based on multi-source information fusion method for key pneumatic units in Chinese standard electric multiple units (EMU) braking system. *Appl. Sci.* **2019**, *9*, 300. [CrossRef]
14. Zhou, D.H.; Ji, H.Q.; He, X.; Shang, J. Fault detection and isolation of the brake cylinder system for Electric Multiple Units. *IEEE Trans. Control. Syst. Technol.* **2018**, *26*, 1744–1757. [CrossRef]
15. Sang, J.X.; Guo, T.X.; Zhang, J.F.; Zhou, D.; Chen, M.; Tai, X. Incipient fault detection for air brake system of high-speed trains. *IEEE Trans. Control. Syst. Technol.* **2021**, *29*, 2026–2037.
16. Ji, H.Q.; Zhou, D.H. Incipient fault detection of the high-speed train air brake system with a combined index. *Control Eng. Pract.* **2020**, *100*, 104425.
17. Ji, H.Q. Statistics Mahalanobis distance for incipient sensor fault detection and diagnosis. *Chem. Eng. Sci.* **2021**, *230*, 116233.
18. Jiang, X.; Zhao, H.; Leung, H. Fault detection and diagnosis in chemical processes using sparse principal component selection. *Ind. Eng. Chem. Res.* **2013**, *52*, 1635–1644.
19. Jian, H.; Yan, X. Dynamic process fault detection and diagnosis based on dynamic principal component analysis, dynamic independent component analysis and bayesian inference. *Chemom. Intell. Lab. Syst.* **2015**, *148*, 115–127.
20. Foster, P. Exploring multivariate data using directions of high density. *Stat. Comput.* **1998**, *8*, 347–355. [CrossRef]
21. Himes, D.M.; Storer, R.H.; Georgakis, C. Determination of the number of principal components for disturbance detection and isolation. *Proc. Am. Control. Conf.* **1994**, *2*, 1279–1283.
22. Ku, W.; Storer, R.H.; Georgakis, C. Disturbance detection and isolation by dynamic principal component analysis. *Chemom. Intell. Lab. Syst.* **1995**, *30*, 176–179.
23. Kourti, T.; Lee, J.; Macgregor, J.F. Experiences with industrial applications of projection methods for multivariate statistical process control. *Comput. Chem. Eng.* **1996**, *20*, 745–750.
24. Li, G.; Alcala, C.F.; Qin, S.J.; Zhou, D. Generalized reconstruction based contributions for output-relevant fault diagnosis with application to the Tennessee Eastman process. *IEEE Trans. Control. Syst. Technol.* **2011**, *19*, 1114–1127.
25. Ding, J.X.; Zuo, J.Y. Fault online simulation of train braking system based on AMESim and LabVIEW. In Proceedings of the 5th International Conference on Mechatronics and Computer Technology Engineering, Chongqing, China, 26–28 August 2022.
26. Ding, J.X. Fault Diagnosis and Prognosis of Air Brake Systems of High-Speed Trains. Ph.D. Thesis, Tongji University, Shanghai, China, 2022.

Disclaimer/Publisher's Note: The statements, opinions and data contained in all publications are solely those of the individual author(s) and contributor(s) and not of MDPI and/or the editor(s). MDPI and/or the editor(s) disclaim responsibility for any injury to people or property resulting from any ideas, methods, instructions or products referred to in the content.